

Integrated valorization of algae residue and oily sludge into hydrogen and liquid biofuels: detailed process simulation and preliminary operational assessment

Marcello Maria Bozzini ^a, Francesco de Fusco ^a, Nuria Ferrera-Lorenzo ^b, Mattia Vallerio ^a, Flavio Manenti ^{a,*}

^a Dipartimento di Chimica, Materiali e Ingegneria Chimica "Giulio Natta" Politecnico di Milano, Piazza Leonardo da Vinci, 32, Milan, 20133, Italy

^b IDENER Chemistry Division, C/ Earle Ovington 24-8, La Rinconada, Seville, 41300, Spain

ARTICLE INFO

Keywords:

BioFuel
Waste-to-X
Microwave pyrolysis
Algae
Sludge

ABSTRACT

The use of biomass for fuel production can considerably reduce the environmental footprint of the energy sector. In this context, microalgae residue and industrial oily sludge emerge as promising feedstocks for the production of sustainable fuels. This work evaluates the technical feasibility and provides a sensitivity analysis of an integrated waste-to-fuel pathway for the co-production of hydrogen and liquid biofuels from waste-derived feedstocks. The pathway combines microwave pyrolysis, reforming and water gas shift of the gaseous fraction, hydrogen-free hydrodeoxygenation of the liquid fraction, and valorization of the solid residue as activated carbon. The same framework is applied to algae residue and oily sludge to assess its robustness toward feedstock variability. Mass and energy balances of the process are derived through Aspen Plus and Aspen HYSYS simulations, allowing the evaluation of key performance indicators. The results show overall energy efficiencies between 41% and 48%, with oily sludge yielding higher liquid fuel production and superior energetic performance. A sensitivity analysis further identifies the hydrocarbon-rich liquid yield and microwave conversion efficiency as the most critical parameters. The results indicate that the proposed process layout represents a promising process configuration for the valorization of waste-derived feedstocks, while co-pyrolysis configurations are left for future investigation.

1. Introduction

Increasing global energy demand and growing concern over the environmental impact of fossil-based fuels are driving the search for more sustainable and efficient processes for biofuel production [1]. In this context, Waste-to-X processes, which convert waste streams into valuable energy carriers and chemicals, are attracting increasing interest in both academia and industry [2]. The combined exploitation of waste resources and renewable energy for the production of advanced biofuels represents a key lever for the ecological transition and the path to decarbonization [3]. According to the Renewable Energy Directive of the European Union, advanced biofuels are expected to contribute at least 5.5% of the final energy consumption in transport by 2030 [4]. In parallel, the United Kingdom is promoting low-carbon fuels in road and aviation through the Renewable Transport Fuel Obligation and the

Sustainable Aviation Fuel Mandate, which require fuel suppliers to blend increasing fractions of sustainable aviation fuel into conventional jet fuel [5]. Multiple biofeedstocks and conversion routes are being investigated, such as lignocellulosic residues or lipid-rich streams, processed via biochemical or thermochemical pathways (gasification, pyrolysis, hydrotreating). Within this framework, feedstocks that are not food competitive and do not compete with arable land are particularly attractive, and they are integrated into the Waste-to-X schemes [6]. In particular, microalgae residues and oily sludge from the dairy industry emerge as promising feedstocks for advanced biofuels owing to their favorable composition and the possibility of coupling waste management with energy production [7]. Within this context, bio-hydrogen is a strategic low-carbon energy carrier and gaseous biofuel whose co-production alongside liquid biofuels can improve process flexibility and overall value generation [8]. In a Waste-to-X perspective,

This article is part of a special issue entitled: SDEWES2025 - RENE published in Renewable Energy.

* Corresponding author.

E-mail address: flavio.manenti@polimi.it (F. Manenti).

<https://doi.org/10.1016/j.renene.2026.125919>

Received 18 December 2025; Received in revised form 1 April 2026; Accepted 7 May 2026

Available online 8 May 2026

0960-1481/© 2026 The Authors. Published by Elsevier Ltd. This is an open access article under the CC BY-NC-ND license (<http://creativecommons.org/licenses/by-nc-nd/4.0/>).

microalgae enable the integration of renewable inputs and marginal resources, as their cultivation is not constrained by arable land availability and can therefore avoid competition with food crops, while offering the potential, under favorable assumptions, for biodiesel yields 50–100 times higher than soybean-based routes [9]. The scale of this opportunity is underlined by reports from the U.S. Department of Energy, which estimate a national production potential of 152 million tons of ash-free dry algal biomass per year. Such a capacity could translate into approximately 14.4 billion gallons of gasoline equivalent annually while capturing 268 million tons of CO₂ [10]. Economically, the sector is experiencing rapid growth; the global microalgae market, valued at USD 3.4 billion in 2020, is projected to reach USD 4.6 billion by 2027, driven by increasing awareness of the functional compounds and sustainability benefits of algae compared to traditional food and energy production methods [11]. Parallel to algal biomass, oily sludge from the dairy industry emerges as a significant feedstock. The European dairy sector processed approximately 144.6 million tons of milk in 2020, 46% more than the United States. This intensive processing generates substantial waste; wastewater treatment in this industry can produce up to 20 kg of dairy processing sludge per m³ of milk processed, resulting in an estimated 2.45 million tons of dairy processing sludge (wet weight) across the EU in 2020 alone [12]. Within this framework and given the results of recent studies, microalgae and oily sludge from the dairy industry emerge as promising candidates to produce biofuels. Also, recent studies have highlighted the potential of algae residues to generate value-added products [13]. Speranza et al. assess algal biodiesel through an area-requirement approach, recommending localized production near demand in climatically suitable areas [14]. Chia et al. review various methods used for converting algal biomass into biofuels, focusing on material yield across different biofuel products [15]. Harman-Ware et al. compare fast pyrolysis of *Scenedesmus* at technical scale, showing bio-oil properties comparable to lignocellulosic pyrolysis but with higher nitrogen content [16]. Previous process-simulation studies on algal thermochemical conversion have mainly relied on equilibrium-based Aspen models for syngas configurations, rather than on integrated pathways for the co-production of hydrogen and liquid biofuels [17]. However, these studies rarely provide fully closed mass and energy balances and an integrated assessment of hydrogen and liquid biofuel co-production into a single simulation framework. The production of biofuels from oily sludge has also been widely investigated at a conceptual level. Zubaidy et al. reviewed several approaches for fuel recovery from fossil oily sludge via solvent extraction [18], while Bora et al. examined the conversion of sewage sludge to biofuel through transesterification [19]. For sludge-derived feedstocks, available process and techno-economic studies have generally focused on pyrolysis for bio-oil production and condensation sections, rather than on a full co-production pathway including hydrogen generation and liquid-fuel upgrading [20]. In parallel, process models for hydrodeoxygenation of biomass-derived liquids have been developed as stand-alone upgrading tools, including applications to bio-oil and algal oil [21]. This work addresses these gaps by investigating an integrated pathway for the production and upgrading of gaseous and liquid biofuels (hydrogen and bio-oil) from algae residue cultivated in domestic wastewater and oily sludge from the dairy industry. In the proposed framework, the two feedstocks are treated as separate case studies, and the same process scheme is applied independently to each feedstock to assess the feasibility of their valorization into hydrogen and liquid biofuels. Microwave (MW) pyrolysis is employed for the thermal decomposition of the feedstocks into gas, liquid and solid fractions. Previous studies have shown that microwave pyrolysis can reduce reaction times and improve product quality compared with conventional heating [22]. Microwave pyrolysis is well-suited for process electrification and intensification, although the benefits depend on the feedstock dielectric properties and reactor scale-up [23]. The pyrolysis gas is subsequently processed using well-established technologies, including catalytic reforming and water–gas shift (WGS) reactors [24]. On the liquid side, the main

objective is to reduce the high oxygen content inherent to the original biomass. This upgrading step is typically energy-intensive and requires large hydrogen inputs, with significant environmental and economic consequences. “Hydrogen-free” hydrodeoxygenation (HDO) has therefore emerged as a promising alternative [25], as it exploits water as the main reactant and eliminates the hydrogen demand of the process [26]. In this context, the novelty of the present work lies in the integrated simulation of a co-production pathway combining microwave pyrolysis, reforming and WGS of the gaseous fraction, hydrogen-free hydrodeoxygenation of the liquid fraction, and activated-carbon valorization of the solid residue. The same framework is then applied to two distinct waste-derived feedstocks, algae residue and oily sludge, to assess its robustness and quantify the effect of feedstock properties on yields, utilities, and overall process performance. In this context, process simulation is essential to derive closed mass and energy balances, quantify utility requirements, and identify integration opportunities at the plant scale [27]. Moreover, a preliminary operational screening is useful to identify the main utility-related cost drivers and to support future, more detailed techno-economic assessments [28]. The main objective of this study is to evaluate the proposed integrated pathway for the co-production of hydrogen and liquid biofuels in terms of material and energy balances, utility requirements and key performance indicators. Co-pyrolysis of the two feedstocks was not considered in the present work, since mixed-feed behavior would require dedicated data on blend-dependent yields and product composition and therefore falls outside the scope of this study. The paper is organized as follows: Section 2 describes the modelling methodology and the selected technologies; Section 3 presents the mass and energy balances for the two feedstock-specific cases; Section 4 discusses the overall energy efficiency and its implications; Section 5 summarizes the main conclusions and outlines future perspectives.

2. Methods

The objective of this study is to propose and evaluate an integrated pathway for the conversion of waste-derived feedstocks into hydrogen and liquid biofuels, considering algae residue and oily sludge as two representative case studies. The process was simulated separately for each feedstock, assuming a feed rate of 100 kg/h of wet feedstock in each case. The key performance parameters include energy efficiency, material yields, and the energy content extracted per kilogram of feedstock. Aspen HYSYS V.14 and Aspen PLUS V.14 were applied for material and energy balance solutions. The same block flow diagram was adopted for both case studies, but no co-feeding or co-pyrolysis configuration was considered in the present work. Fig. 1 shows the Block Flow Diagram (BFD) of the process. Firstly, the feedstock is introduced into the microwave (MW) pyrolysis reactor to produce pyrolysis gas, a crude bio-liquid and solid residue (biochar). The pyrolysis gas is sent to a separator to remove condensable molecules, mainly ammonia and water, and compressed before entering the gas reforming section. Finally, Water Gas Shift (WGS) reactors are implemented to maximize hydrogen production. The bio-liquid contains a high amount of oxygen-based molecules, which must be refined to produce liquid biofuels. Hence, this fraction is sent to the “hydrogen-free” hydrodeoxygenation section for the upgrading of the oxygenated liquid fraction into a hydrocarbon-rich liquid fuel. Finally, the solid fraction is exploited for the production of activated carbon via physical activation with CO₂, which can be used as a microwave susceptor in the MW pyrolysis reactor [29]. The energy content of the upgraded liquid biofuel was evaluated using the lower heating values (LHV) of the representative products selected for the liquid product (44.4 MJ/kg for octane and 47.2 MJ/kg for hexane).

2.1. Feedstock characterization

The first feedstock considered in this work is algae residue recovered

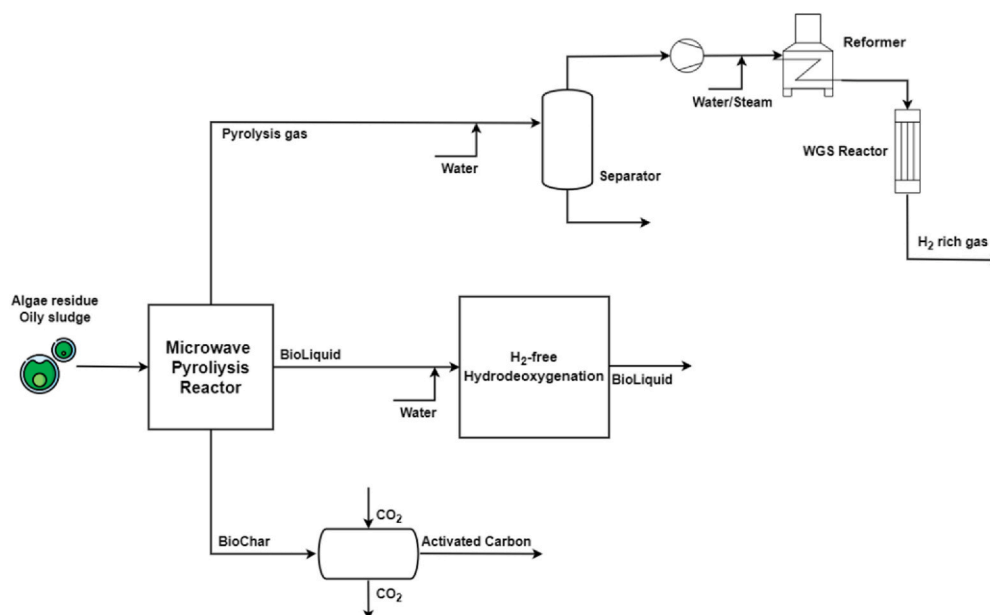


Fig. 1. Block Flow Diagram of the proposed process.

after cultivation in domestic wastewater. The second feedstock is an oily sludge generated in dairy-processing facility. Table 1 shows the proximate and ultimate analyses of algae residue and oily sludge feedstocks reported on a dry basis [30]. Humidity quantifies the water content of the wet feedstock. It is assumed that both feedstocks are partially dried to a moisture content of 10%. The drying step is not explicitly modeled in the process flowsheet because its energy demand strongly depends on the selected drying technology and heat-integration strategy. A drying energy demand contribution of 3.2 MJ per kg of evaporated water was assumed for the operational screening [31]. Also, the oxygen content was determined by difference and not directly analyzed. As illustrated, the oily sludge feedstock has lower humidity content and higher carbon and hydrogen fractions. The significant presence of nitrogen and oxygen in both feedstocks results in the formation of highly oxygenated and nitrogen-containing products. These marked differences in physico-chemical properties make algae residue and oily sludge suitable representative case studies to assess the applicability of the proposed integrated pathway to distinct waste-derived streams.

2.2. Microwave pyrolysis unit

The MW pyrolysis reactor operates in continuous mode at 2 bar to avoid oxygen infiltration during the process, while the feedstock enters at ambient temperature (i.e., 25 °C) and exits at 700 °C. The resulting product streams are then released to atmospheric pressure before entering the downstream cooling and separation sections. The corresponding inlet streams of the post-processing sections are reported at 1.01 bar in the appendix tables. The separation of the pyrolysis gas, bio-liquid and biochar is performed within the MW reactor. The MW duty reported refers to the effective microwave power absorbed by the feedstock to reach the target pyrolysis conditions. To estimate the corresponding electrical power demand, a nominal conversion efficiency of 0.70 was assumed. A sensitivity analysis was additionally considered to account for generator performance and system-level losses reported in

the literature [32]. The pyrolysis products were not predicted through a detailed kinetic model. Instead, a reduced-order, feedstock-specific approach was adopted to reconstruct a representative product slate for process simulation. First, the proximate and ultimate analyses of each feedstock were used to define the elemental composition of the non-conventional material. Second, literature data under comparable pyrolysis conditions were used to define the overall distribution among gas, liquid and solid fractions, as well as the dominant chemical families in the volatile products. Third, each phase was represented by a limited set of surrogate compounds, reported in Table 2, selected to reproduce the main species families relevant for downstream upgrading. For the bio-liquid fraction, the selected surrogates were chosen to represent nitrogen-containing aromatics, oxygenated compounds and light hydrocarbons. Finally, the flow rates of the surrogate species were obtained by solving elemental balances for C, H, O and N, thus ensuring mass-balance consistency between the original feedstock and the reconstructed pyrolysis products. The elemental distribution among the three pyrolysis fractions was derived from the literature basis adopted for each feedstock, while the thermodynamic properties of the non-conventional feedstock were estimated through the Non-Conventional Component Tool using the proximate and ultimate analyses reported in Table 1 [33]. For algae residue, the

Table 2

Surrogate compounds adopted for modelling the gas and liquid pyrolysis fractions.

Surrogate compounds	
Gas phase	Liquid phase
H ₂	Pyrrole
CH ₄	C ₈ H ₁₄ O ₄
CO	Benzene
CO ₂	Toluene
NH ₃	C ₆ H ₁₄

Table 1

Total humidity, proximate and ultimate analysis of both feedstocks.

Biomass Waste	Humidity (%)	VM Ash (%) (%)	C (%)	H (%)	N (%)	S (%)	O (%)
Algae residue	84.3	62.98 22.26	41.73	6.19	4.10	0.25	25.47
Oily sludge	75.9	79.8 13.35	54.31	8.45	5.88	0.38	17.63

surrogate-product definition was derived from experimental studies on algal and microalgal pyrolysis reporting phase yields and representative bio-oil compounds [34], [35]. For the second feedstock, the literature basis was aligned with studies on pyrolysis of milk/dairy processing sludge, which report significant liquid production together with gas-phase nitrogen species such as NH_3 and HCN [36], [37]. The resulting product distribution should therefore be interpreted as a thermodynamically consistent lumped representation, rather than as a detailed prediction of the exact molecular composition of the actual pyrolysis products. Material balances were implemented in Microsoft Excel, while the corresponding energy balances were solved in Aspen Plus V.14.

2.3. Pyrolysis gas post-processing section

Aspen HYSYS V.14 was used to perform the simulation of the process. The Soave-Redlich-Kwong (SRK) equation of state was chosen to model the mixture behavior as it is recommended for petrochemical operations [38]. Fig. 2 presents the process flow diagram of the post-processing section of the pyrolysis gas. Initially, the hot pyrolysis stream (stream 1) is brought into contact with a water stream (stream 2), which reduces its temperature from 700 °C to 70 °C. The cooled mixture is then sent to heat exchanger E-101, where it is further cooled down to 30 °C. This temperature drop allows for the removal of water and ammonia in the downstream separator V-101 (stream 5). Although sulfur is present in the original feedstocks, sulfur-containing gas species were not explicitly included in the surrogate pyrolysis-gas model. Therefore, the gas-upgrading section should be interpreted as an idealized sulfur-free case, and the possible need for dedicated desulfurization and catalyst-protection steps is not captured in the present simulation. The conditioned gas (stream 6) is then pressurized to 4 bar with compressor K-101, aligning with the operating pressure required by the reforming unit (R-101) as a representative process value for the subsequent handling of the hydrogen-rich gas stream. No dedicated hydrogen-purification step was explicitly modeled in the present work. Before entering the reformer, the gas is mixed with steam (stream 8) and passed through a process-to-process heat exchanger (E-102), which recovers heat from the reformer outlet stream (stream 11) to preheat the incoming mixture (stream 10). The reformer operates at 900 °C, a temperature at which the steam reforming reactions are assumed to reach thermodynamic equilibrium [18], consistent with high temperature reforming conditions to favor equilibrium conversion. The reformed gas is cooled to 250 °C in E-103 using water as a cooling medium. This temperature is suitable for the first adiabatic water-gas shift reactor (R-102). The output gas (stream 14) is subsequently cooled once more to 250 °C and directed to a second adiabatic WGS reactor (R-103) [39]. The final hydrogen-rich gas stream (stream 16) is characterized in terms of composition and lower heating value, but no downstream hydrogen-purification is explicitly modeled. The energetic contribution of stream 16 was evaluated on an LHV basis considering the

combustible components of the hydrogen-rich gas. Table 3 reports the temperatures and pressures of the input streams. The reforming and WGS reactors were modeled under thermodynamic equilibrium assumptions, given that the reactions are primarily constrained by thermodynamics. The water mass flow rate of stream 2 was selected to achieve the desired temperature in stream 3 after mixing, while the steam flow of stream 8 was adjusted to maintain a steam-to-carbon ratio of 3 [40].

2.4. Bio-liquid refining section

Fig. 3 shows the bio-liquid refining PFD. The bio-liquid obtained from the microwave pyrolysis reactor (stream 17) is initially combined with water (stream 18) to reduce the temperature of the mixture. Stream 19 is then cooled further to 60 °C in heat exchanger E-105 using cooling water. The condensed output (stream 20) is pressurized to 16 bar by pump P-101 to match the operating pressure required for the "hydrogen-free" hydrodeoxygenation (HDO) process described in the work of Jin et al. [25], resulting in stream 21. The liquid-upgrading section was not intended to represent a detailed reaction-resolved HDO mechanism. Instead, it was formulated as a simplified surrogate-based upgrading block inspired by H_2 -free hydrodeoxygenation concepts reported in the literature. In this representation, process water is introduced as a reaction medium, and the upgrading step is modeled as the conversion of the oxygenated bio-liquid into a hydrocarbon-rich fuel fraction together with an aqueous by-product stream and a residual heteroatomic non-fuel fraction. Therefore, nitrogen-containing compounds represented by pyrrole are excluded from the upgraded-fuel energy content.

The output of the upgrading block (stream 22) then undergoes a separation step to isolate the hydrocarbon-rich liquid fuel fraction (stream 26) from a non-fuel by-product stream (stream 25), which includes the separated aqueous and heteroatomic residual species. The energetic contribution of the liquid product was quantified on a lower heating value basis, without introducing any downstream conversion unit. The fixed input parameters used for the simulation of this process are detailed in Table 4.

Table 3
Input parameters for pyrolysis gas post-processing in Aspen HYSYS simulation.

Stream Number	Temperature [°C]	Pressure [bar]
1	700	2
2	30	2
3	70	-
4	30	-
7	-	4
10	500	-
11	900	-
13	250	-
15	250	-

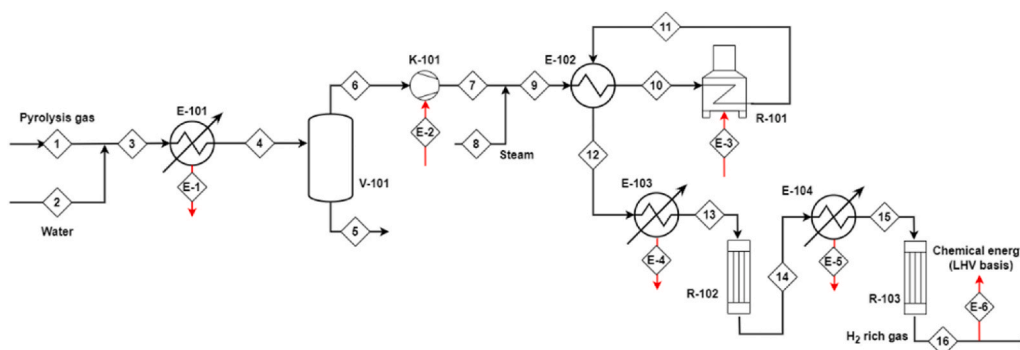


Fig. 2. Process Flow Diagram of pyrolysis gas post-processing.

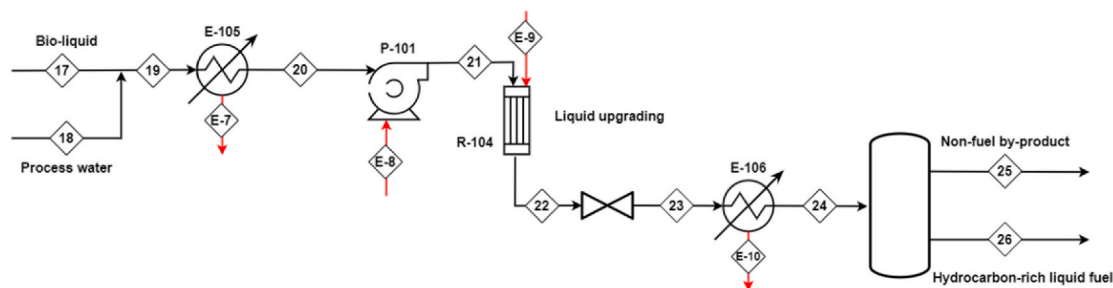


Fig. 3. Process Flow Diagram of Bio-liquid refining section.

Table 4

Input parameters for Bio-liquid refining section in Aspen HYSYS simulation.

Stream Number	Temperature [°C]	Pressure [bar]
17	700	1.01
18	30	1.01
20	60	1.01
21	-	16
22	250	16
23	-	2
24	50	2

2.5. Sensitivity

To account for the uncertainties inherent in the analysis in this study and to identify the primary drivers of performance, a sensitivity analysis was conducted on both the algae residue and oily sludge pathways by varying each key variable from its baseline value while keeping all other parameters constant. The analysis evaluates how a variation of $\pm 10\%$ and $\pm 20\%$ in key operational parameters and product yields affects the overall energy efficiency of the system. The parameters considered include the drying duty required and hot thermal duty to assess the impact of feedstock moisture and thermal integration, nominal microwave conversion efficiency varying from the baseline of 0.7, and the yields of hydrogen-rich gaseous fuel and hydrocarbon-rich liquid fuel, which directly influence the energy recovery potential of the plant. The target output for this analysis is the overall energy efficiency, defined as the ratio between the energy content of the upgraded biofuels and the total electrical and thermal energy supplied to the process. This methodology allows for a direct comparison between the two feedstocks, highlighting which operational area (e.g., drying vs. reaction yield) offers the greatest margin for efficiency optimization.

3. Results and discussion

This section is organized into two main parts, each focusing on one of the feedstocks analyzed in the study. The first part includes the process datasheet and the corresponding energy and mass balances for the algae residue feedstock. A similar approach is then applied to the oily sludge feedstock. The simulations are based on a wet feedstock input of 100 kg/h. A final comparative analysis of the two case studies, highlighting product yields, utility consumptions and overall process performance is presented.

3.1. Algae residue feedstock

Table 6 shows the reconstructed distribution of the three output fractions for the algae-residue case in the process simulation. The remaining fraction, totaling 84.2 kg/h, is composed primarily of vapor derived from the high initial moisture content of the wet feedstock (see Table 1). The power delivered to the algae feedstock is equal to 37 kW, which corresponds to an overall electrical demand of 53 kW. These reconstructed output streams were subsequently imported into Aspen

Table 6

Reconstructed pyrolysis product slate for the algae-residue case used in the downstream process simulation.

Pyrolysis gas		Bio-liquid		biochar	
Component	Mass Flow [kg/h]	Component	Mass Flow [kg/h]	Component	Mass Flow [kg/h]
Hydrogen	0.1109	Pyrrole	1.3863	Char	2.1042
CO ₂	1.5406	C ₈ H ₁₄ O ₄	5.9794	Ash	3.5300
CO	0.5311	Toluene	0.0537		
Methane	0.1984				
Ammonia	0.3502				
Total	2.7311	Total	7.4194	Total	5.6442

HYSYS for downstream processing.

Table A.13 shows the datasheet of the pyrolysis gas post-processing section with the algae feedstock. The reforming section is able to completely convert methane into hydrogen. Finally, the WGS reactors reduce the CO content from 0.26 to 0.08 in molar fraction, maximizing the hydrogen content of the final product. The post-processing of the pyrolysis gas led to a production of 0.22 kg/h of hydrogen, starting from 100 kg/h of wet feedstock. The energetic content of the hydrogen-rich gas stream was quantified on an LHV basis by considering the combustible components present in the stream. For the representative composition reported here, the corresponding energy content amounts to 8.27 kW.

Table A.14 shows the datasheet of the bio-liquid refining section. The core of this section is the "hydrogen-free" dehydrogenation reactor, which refines the oxygenated molecule to give a hydrocarbon-rich liquid fuel. Processing the crude bio-liquid obtained from microwave pyrolysis yields approximately 4.1 kg/h of hydrocarbon-rich liquid fuel. The upgraded liquid biofuel has an estimated energetic content of 50.45 kW on an LHV basis. Finally, assuming a mass loss of 50 % of the initial char, the production of activated carbon is estimated to be approximately 1.05 kg/h. Finally, Table 7 summarizes the energy streams associated with the post-processing of pyrolysis gas and the upgrading of the bio-liquid. Notably, E-2 and E-8 correspond to electrical energy inputs, whereas negative values denote energy removal from the system through cooling.

3.2. Oily sludge feedstock

Table 8 reports the reconstructed distribution of the three product fractions for the oily sludge feedstock. The vapor fraction accounts for

Table 7

Energy streams of the process (see Figs. 2 and 3 for stream numbers).

Energy stream	E-1	E-2	E-3	E-4	E-5
Heat flow [kW]	-1.16	0.09	1.64	-0.68	-0.27
Energy stream	E-6	E-7	E-8	E-9	E-10
Heat flow [kW]	8.27	-4.06	0.01	14.04	-1.31

Table 8

Reconstructed pyrolysis product slate for the oily sludge case used in the downstream process simulation.

Pyrolysis gas		Bio-liquid		biochar	
Component	Mass Flow [kg/h]	Component	Mass Flow [kg/h]	Component	Mass Flow [kg/h]
Hydrogen	0.1117	Pyrrole	3.0518	Char	3.8523
CO ₂	0.6655	C ₈ H ₁₄ O ₄	6.3533	Ash	3.3100
CO	1.8352	Benzene	0.6301		
Methane	0.8470	C ₆ H ₁₄	2.6689		
Ammonia	0.7752				
Total	4.2347	Total	12.7041	Total	7.1623

75.9 kg/h, consistent with the high moisture content of the original feedstock reported in Table 1. The microwave pyrolysis unit is associated with an absorbed MW duty of 88 kW, which corresponds to an overall electrical demand of 125.7 kW. These reconstructed output streams were used as input for downstream processing.

Table A.15 illustrates the datasheet of the pyrolysis gas post-processing section with the sludge feedstock. Post-processing yields roughly 0.59 kg/h of hydrogen from an initial input of 100 kg/h of wet feedstock. The energetic contribution of the final hydrogen-rich gas stream, evaluated on a lower-heating-value basis by considering the combustible species present, is estimated at 21.93 kW. Table A.16 reports the datasheet of the bio-liquid refining section for the oily sludge case. The simplified liquid-upgrading block converts the oxygenated bio-liquid into a hydrocarbon-rich liquid fuel fraction. The upgraded liquid fuel has an energetic content of 80.16 kW on an LHV basis. Concerning the valorization of char, assuming a 50% mass loss of the solid residue, the production of activated carbon is estimated to be approximately 1.92 kg/h. Table 9 provides an overview of the energy flows involved in both the pyrolysis gas post-treatment and the bio-liquid refining stages.

3.3. Process performance assessment

Table 10 illustrates the main input and output material and energy streams for the two cases. The energetic content of the gaseous and liquid products is reported on an LHV basis. The gaseous product refers to the hydrogen-rich gas stream, and the H₂ value indicates the hydrogen content contained in that stream rather than purified hydrogen. The MW pyrolysis reactor is the most energy-intensive unit of the process. Since both feedstocks are assumed to be pre-dried to 10 wt% moisture, 82.6 kg/h and 73.2 kg/h of water must be removed from algae residue and oily sludge before entering the pyrolysis step. The corresponding drying duty, estimated assuming a nominal specific drying energy of 3.2 MJ per kg of evaporated water, is included in Table 10. Based on the pre-dried feed input, the absorbed MW energy requirement is 7.6 MJ per kg of feed at 10 wt% moisture for algae residue and 11.8 MJ per kg for oily sludge. The higher energy demand of the second feedstock is consistent with its lower ash content and higher carbon fraction. As shown in Table 10, the oily sludge feedstock has higher product yields on a wet basis with respect to the algae residue feedstock, mainly because of its lower initial moisture content. When both the hydrogen-rich gas stream and the hydrocarbon-rich liquid fuel are considered on an LHV basis, the total energy recovered in the products is 12.0 MJ per kg of feed at 10 wt% moisture for algae residue and 13.7 MJ

Table 9

Energy streams of the process (see Figs. 2 and 3 for stream numbers).

Energy stream	E-1	E-2	E-3	E-4	E-5
Heat flow [kW]	-2.10	0.13	4.67	-1.71	-0.85
Energy stream	E-6	E-7	E-8	E-9	E-10
Heat flow [kW]	21.93	-7.07	0.01	15.94	-2.38

Table 10

Input and output material and energy streams for the two feedstock-specific cases.

	Input		Output	
	Algae residue	Oily Sludge	Algae residue	Oily Sludge
Wet Feedstock	100 [kg/h]	100 [kg/h]		
Drying duty [kW]	73.4	65.1		
Cold thermal duty [kW]	7.48	14.11		
Hot thermal duty [kW]	15.68	20.61		
Electrical demand [kW]	53.1	125.8		
Hydrogen-rich gaseous fuel			8.27 kW	21.93 kW
Hydrocarbon-rich liquid fuel			4.10 kg/h	6.53 kg/h
CO ₂ (dir. em.)			50.45 kW	80.16 kW
			2.78 kg/h	5.53 kg/h

per kg for oily sludge. Regarding the energy efficiency of the processes, the algae feedstock requires more power (hot thermal and electric) per unit of recovered product energy. In particular, the energy efficiency for the algae residue feedstock is 41.4%, while for the oily sludge feedstock, it stands at 48.3%. A concise comparison of the two feedstocks is reported in Table 11, which highlights the higher hydrocarbon-rich liquid yield and the more favorable overall energetic performance of oily sludge.

3.4. Sensitivity

The results of the sensitivity analysis are illustrated in the sensitivity plots (Fig. 4) for algae residue and oily sludge. The results reveal several critical trends. The overall energy efficiency is most sensitive to the yield of hydrocarbon-rich liquid fuel. A 20% increase in this yield pushes the energy efficiency toward 49% for algae and nearly 56% for oily sludge. This highlights that the liquid biofuel fraction is the dominant energy carrier in the proposed layout. The nominal conversion efficiency of the microwave shows that improving the efficiency of the electrical-to-microwave power conversion is a vital lever for increasing the viability of the "Waste-to-X" scheme. The drying duty exhibits a strong inverse relationship with energy efficiency. Given the high initial moisture content of the feedstocks (84.3% for algae and 75.9% for sludge), reductions in drying energy, potentially through advanced mechanical dewatering or heat integration, result in substantial efficiency gains. Finally, while the hydrogen-rich gaseous fuel contributes positively to the energy balance, its impact on total efficiency is less pronounced than that of the liquid fraction, reflecting its secondary role in the products. The sensitivity profiles for both feedstocks follow a similar pattern. However, the oily sludge case maintains a higher baseline efficiency across all variations, primarily due to its superior carbon and hydrogen content and lower initial humidity compared to the algae residue. This analysis highlights that while both pathways are technically feasible, optimization efforts should prioritize the enhancement of liquid fuel recovery and the reduction of drying-related energy

Table 11

Key performance indicators for the two feedstock-specific cases.

Parameter	Algae residue	Oily sludge
Feed input at 10 wt% moisture [kg/h]	17.6	26.8
MW pyrolysis absorbed energy [MJ/kg _{feed} at 10 wt% moisture]	7.6	11.8
Energy in products [MJ/kg _{feed} at 10 wt% moisture]	12.0	13.7
H ₂ production [kg/h]	0.22	0.59
Hydrocarbon-rich liquid fuel [kg/h]	3.93	6.53
Activated carbon [kg/h]	1.05	1.92
Direct CO ₂ emissions [kg/h]	2.78	5.53
Energy efficiency [%]	41.4%	48.3%

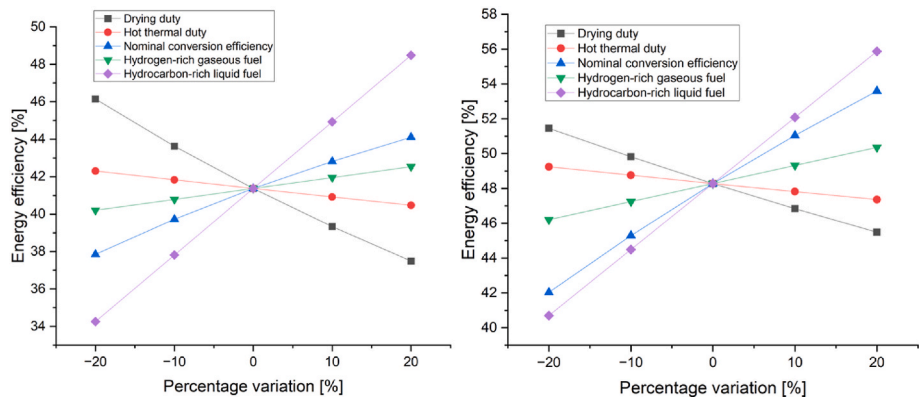


Fig. 4. Sensitivity plot of algae residue (left) and oily sludge (right) feedstock.

expenditure.

4. Conclusions

This study focuses on the development of a detailed process simulation for the conversion of algae residue and oily sludge into hydrogen and liquid biofuels via microwave pyrolysis and post-processing of pyrolysis gas and bio-liquid. The same process scheme was applied separately to the two feedstocks in order to assess the technical feasibility of their conversion and quantify the associated material and energy balances. The overall energy efficiency of the processes ranges between 41% and 48%, with the oily sludge showing higher biofuel yield on a dry basis and overall higher energetic performance. A local sensitivity analysis further clarifies the process dynamics, identifying the hydrocarbon-rich liquid fuel yield and the nominal microwave conversion efficiency as the most influential parameters on the global energy performance. Overall, the promising key process parameters suggest that the exploitation of such wastes can be feasible from both technical and economic points of view. The identification of bottlenecks or possible impurities (oxygen- or sulfur-based compounds) in the pyrolysis products is crucial to avoid potential catalyst deactivation during pyrolysis gas post-processing and bio-liquid refining. The preliminary operational screening shows that the process performance is strongly affected by electricity-related demand, particularly drying and microwave-assisted conversion. Overall, the proposed integrated pathway represents a promising option for the valorization of low-value waste streams into higher-value energy carriers. Future developments should focus on the availability of experimental data to further refine the simulation, the identification of impurities and bottlenecks that may affect catalyst stability during gas and liquid upgrading, and the optimization of process parameters to improve material and energy efficiency. However, it should be noted that extrapolation of MW power demand beyond laboratory or pilot scale remains uncertain, because microwave-assisted pyrolysis still faces scale-up challenges related to field uniformity, penetration depth, dielectric-property dependence, and

continuous-feed reactor design. In addition, the availability of dedicated experimental data could enable future assessment of mixed-feed co-processing strategies, including co-feeding or co-pyrolysis of selected waste streams.

CRediT authorship contribution statement

Marcello Maria Bozzini: Conceptualization, Data curation, Formal analysis, Investigation, Methodology, Writing – original draft, Writing – review & editing. **Francesco de Fusco:** Data curation, Formal analysis, Methodology, Writing – original draft, Writing – review & editing. **Nuria Ferrera-Lorenzo:** Conceptualization, Data curation, Methodology, Writing – original draft. **Mattia Vallerio:** Conceptualization, Data curation, Writing – original draft, Writing – review & editing. **Flavio Manenti:** Conceptualization, Funding acquisition, Methodology, Supervision, Writing – original draft, Writing – review & editing.

Declaration of competing interest

The authors declare that they have no known competing financial interests or personal relationships that could have appeared to influence the work reported in this paper.

Acknowledgments

Funded by the European Union. Views and opinions expressed are however those of the author(s) only and do not necessarily reflect those of the European Union or CINEA. Neither the European Union nor the granting authority can be held responsible for them. The work described in this publication was subsidised by Horizon Europe (HORIZON) framework through the Grant Agreement Number 101144144.

A preliminary version of this work was presented at the 20th SDEWES Conference, held from 5 to 10 October 2025 in Dubrovnik, Croatia.

Appendix A. Datasheet

Table A.13
Pyrolysis gas post-processing datasheet (see Fig. 2 for stream numbers, algae feedstock)

Stream number	1	2	3	4	5	6	7	8
Vapor Fraction	1	0	0.422	0.285	0	1	1	1
Temperature [°C]	700	30	70	30	30	30	195	250
Pressure [bar]	1.01	1.01	1.01	1.01	1.01	1.01	4.00	4.00
Molar Flow [kmol/h]	0.14	0.33	0.47	0.47	0.35	0.12	0.12	0.04

(continued on next page)

Table A.13 (continued)

Mass Flow [kg/h]	2.73	5.90	8.63	8.63	6.25	2.38	2.38	0.67
Molar fraction								
Hydrogen	0.39	0.00	0.12	0.12	0.00	0.45	0.45	0.00
CO ₂	0.25	0.00	0.07	0.07	0.00	0.29	0.29	0.00
CO	0.13	0.00	0.04	0.04	0.00	0.16	0.16	0.00
Methane	0.09	0.00	0.03	0.03	0.00	0.10	0.10	0.00
Ammonia	0.14	0.00	0.04	0.04	0.94	0.00	0.00	0.00
Water	0.00	1.00	0.70	0.70	0.06	0.00	0.00	1.00
Stream number	9	10	11	12	13	14	15	16
Vapor Fraction	1	1	1	1	1	1	1	1
Temperature [°C]	208	500	900	642	250	406	250	299
Pressure [bar]	4.00	4.00	4.00	4.00	4.00	4.00	4.00	4.00
Molar Flow [kmol/h]	0.16	0.16	0.18	0.18	0.18	0.18	0.18	0.18
Mass Flow [kg/h]	3.05	3.05	3.05	3.05	3.05	3.05	3.05	3.05
Molar fraction								
Hydrogen	0.35	0.35	0.42	0.42	0.42	0.55	0.55	0.59
CO ₂	0.22	0.22	0.11	0.11	0.11	0.24	0.24	0.28
CO	0.12	0.12	0.26	0.26	0.26	0.12	0.12	0.08
Methane	0.08	0.08	0.00	0.00	0.00	0.00	0.00	0.00
Ammonia	0.14	0.00	0.00	0.00	0.00	0.00	0.00	0.00
Water	0.23	0.23	0.22	0.22	0.22	0.09	0.09	0.05

Table A.14

Bio-liquid refining datasheet (see Fig. 3 for stream numbers, algae feed-stock)

Stream Number	17	18	19	20	21
Vapor Fraction	1	0	1	0	0
Temperature [°C]	700	30	473	60	60
Pressure [bar]	1.01	1.01	1.01	1.01	16.00
Molar Flow [kmol/h]	0.06	0.07	0.12	0.12	0.12
Mass Flow [kg/h]	7.42	1.24	8.66	8.66	8.66
Molar fraction					
Pyrrole	0.37	0.00	0.17	0.17	0.17
Toluene	0.01	0.00	0.00	0.00	0.00
C ₈ H ₁₄ O ₄	0.62	0.00	0.28	0.28	0.28
C ₈ H ₁₈	0.00	0.00	0.00	0.00	0.00
C ₆ H ₁₄	0.00	0.00	0.00	0.00	0.00
Water	0.00	1.00	0.55	0.55	0.55
Stream Number	22	23	24	26	
Vapor Fraction	1	1	0	0	
Temperature [°C]	250	243	50	50	
Pressure [bar]	16.00	2.00	2.00	2.00	
Molar Flow [kmol/h]	0.16	0.16	0.16	0.036	
Mass Flow [kg/h]	8.66	8.66	8.66	4.10	
Molar fraction					
Pyrrole	0.13	0.13	0.13	0.00	
Toluene	0.00	0.00	0.00	0.02	
C ₈ H ₁₄ O ₄	0.00	0.00	0.00	0.00	
C ₈ H ₁₈	0.22	0.22	0.22	0.98	
Water	0.65	0.65	0.65	0.00	

Stream 25 represents an aggregated non-fuel by-product stream including process water and residual heteroatomic species. Its detailed composition was not further resolved in the present simplified upgrading model.

Table A.15

Pyrolysis gas post-processing datasheet (see Fig. 2 for stream numbers, oily sludge feedstock)

Stream number	1	2	3	4	5	6	7	8
Vapor Fraction	1	0	0.333	0.217	0	1	1	1
Temperature [°C]	700	30	70	30	30	30	198	250
Pressure [bar]	1.01	1.01	1.01	1.01	1.01	1.01	4.00	4.00
Molar Flow [kmol/h]	0.24	0.72	0.96	0.96	0.77	0.18	0.18	0.15
Mass Flow [kg/h]	4.24	13.00	17.24	17.24	13.86	3.38	3.38	2.79
Molar fraction								
Hydrogen	0.23	0.00	0.06	0.06	0.00	0.29	0.29	0.00
CO ₂	0.06	0.00	0.02	0.02	0.00	0.08	0.08	0.00
CO	0.27	0.00	0.07	0.07	0.00	0.35	0.35	0.00
Methane	0.22	0.00	0.05	0.05	0.00	0.28	0.28	0.00
Ammonia	0.21	0.00	0.05	0.05	0.07	0.00	0.00	0.00
Water	0.00	1.00	0.75	0.75	0.93	0.00	0.00	1.00
Stream number	9	10	11	12	13	14	15	16
Vapor Fraction	1	1	1	1	1	1	1	1
Temperature [°C]	221	500	900	671	250	393	250	293

(continued on next page)

Table A.15 (continued)

Pressure [bar]	4.00	4.00	4.00	4.00	4.00	4.00	4.00	4.00
Molar Flow [kmol/h]	0.34	0.34	0.44	0.44	0.44	0.44	0.44	0.44
Mass Flow [kg/h]	6.17	6.17	6.17	6.17	6.17	6.17	6.17	6.17
Molar fraction								
Hydrogen	0.16	0.16	0.50	0.50	0.50	0.62	0.62	0.66
CO ₂	0.04	0.04	0.07	0.07	0.07	0.19	0.19	0.22
CO	0.19	0.19	0.22	0.22	0.22	0.10	0.10	0.07
Methane	0.15	0.15	0.00	0.00	0.00	0.00	0.00	0.00
Ammonia	0.00	0.00	0.00	0.00	0.00	0.00	0.00	0.00
Water	0.46	0.46	0.20	0.20	0.20	0.08	0.08	0.04

Table A.16

Bio-liquid refining datasheet (see Fig. 3 for stream numbers, oily sludge feedstock)

Stream Number	17	18	19	20	21
Vapor Fraction	1	0	1	0	0
Temperature [°C]	700	30	567	60	60
Pressure [bar]	1.01	1.01	1.01	1.01	16.00
Molar Flow [kmol/h]	0.12	0.07	0.19	0.19	0.19
Mass Flow [kg/h]	12.70	1.31	14.02	14.02	14.02
Molar fraction					
Pyrrrole	0.38	0.00	0.23	0.23	0.23
Benzene	0.07	0.00	0.04	0.04	0.04
C ₈ H ₁₄ O ₄	0.30	0.00	0.19	0.19	0.19
C ₈ H ₁₈	0.00	0.00	0.00	0.00	0.00
C ₆ H ₁₄	0.26	0.00	0.16	0.16	0.16
Water	0.00	1.00	0.38	0.38	0.38
Stream Number	22	23	24	26	
Vapor Fraction	1	1	0	0	
Temperature [°C]	250	243	50	50	
Pressure [bar]	16.00	2.00	2.00	2.00	
Molar Flow [kmol/h]	0.23	0.23	0.23	0.065	
Mass Flow [kg/h]	14.02	14.02	14.02	6.53	
Molar fraction					
Pyrrrole	0.20	0.20	0.20	0.00	
Benzene	0.04	0.04	0.04	0.10	
C ₈ H ₁₄ O ₄	0.00	0.00	0.00	0.00	
C ₈ H ₁₈	0.16	0.16	0.16	0.54	
C ₆ H ₁₄	0.13	0.13	0.13	0.36	
Water	0.47	0.47	0.47	0.00	

Stream 25 represents an aggregated non-fuel by-product stream including process water and residual heteroatomic species. Its detailed composition was not further resolved in the present simplified upgrading model.

References

- [1] F. Tan, W. Lu, B. Cao, S. Wang, M. Mu, A. Zheng, Environmental impact and water footprint of biofuel production from macro-algae biomass based on life cycle assessment, *Renew. Energy* 254 (Dec. 2025) 123612, <https://doi.org/10.1016/j.renene.2025.123612>.
- [2] N. Sifakis, N. Savvakis, M. Petropoulou, G. Arampatzis, Techno-economic optimization of a novel industrial hybrid renewable energy system based on the waste-to-X principle, *Energy Convers. Manag.* 313 (Aug. 2024) 118613, <https://doi.org/10.1016/j.enconman.2024.118613>.
- [3] E. Bocci, et al., Biomass to fuel cells state of the art: a review of the most innovative technology solutions, *Int. J. Hydrogen Energy* 39 (36) (Dec. 2014) 21876–21895, <https://doi.org/10.1016/j.ijhydene.2014.09.022>.
- [4] Direttiva (UE) 2023/2413 Del Parlamento Europeo E Del Consiglio, Del 18 Ottobre 2023, Che Modifica La Direttiva (UE) 2018/2001, Il Regolamento (UE) 2018/1999 E La Direttiva N. 98/70/CE per Quanto Riguarda La Promozione Dell'Energia Da Fonti Rinnovabili E Che Abroga La Direttiva (UE) 2015/652 Del Consiglio'.
- [5] RTFO and SAF Mandate Technical Guidance, 2025.
- [6] P.A. Østergaard, P. Cabrera, R.M. Johannsen, N. Duic, S. Kalogirou, Advancing sustainability through renewable energy technologies: trends and innovations, *Renew. Energy* 255 (Dec. 2025) 124595, <https://doi.org/10.1016/j.renene.2025.124595>.
- [7] O.M. Adeniyi, U. Azimov, A. Burluka, Algae biofuel: current status and future applications, *Renew. Sustain. Energy Rev.* 90 (Jul. 2018) 316–335, <https://doi.org/10.1016/j.rser.2018.03.067>.
- [8] C. Mansilha, A. Barbosa-Póvoa, L. Tarelho, A. Fonseca, A comprehensive review of green hydrogen production technologies: current status, challenges, research trends and future directions, *Renew. Sustain. Energy Rev.* 225 (Jan. 2026) 116119, <https://doi.org/10.1016/j.rser.2025.116119>.
- [9] B.J. Gallagher, The economics of producing biodiesel from algae, *Renew. Energy* 36 (1) (Jan. 2011) 158–162, <https://doi.org/10.1016/j.renene.2010.06.016>.
- [10] R. Davis, et al., Economic, Greenhouse Gas, and Resource Assessment for Fuel and Protein Production from Microalgae: 2022 Algae Harmonization Update, 2024, <https://doi.org/10.2172/2318964>.
- [11] P. Loke Show, Global market and economic analysis of microalgae technology: status and perspectives, *Bioresour. Technol.* 357 (Aug. 2022) 127329, <https://doi.org/10.1016/j.biortech.2022.127329>.
- [12] Y. Hu, et al., Systematic review of dairy processing sludge and secondary STRUBIAS products used in agriculture, *Front. Sustain. Food Syst.* 5 (Nov. 2021), <https://doi.org/10.3389/fsufs.2021.763020>.
- [13] Y.-D. Chen, F. Liu, N.-Q. Ren, S.-H. Ho, Revolutions in algal biochar for different applications: state-of-the-art techniques and future scenarios, *Chin. Chem. Lett.* 31 (10) (Oct. 2020) 2591–2602, <https://doi.org/10.1016/j.cclet.2020.08.019>.
- [14] L.G. Speranza, A. Ingram, G.A. Leeke, Assessment of algae biodiesel viability based on the area requirement in the European Union, United States and Brazil, *Renew. Energy* 78 (Jun. 2015) 406–417, <https://doi.org/10.1016/j.renene.2014.12.059>.
- [15] S.R. Chia, et al., Sustainable approaches for algae utilisation in bioenergy production, *Renew. Energy* 129 (Dec. 2018) 838–852, <https://doi.org/10.1016/j.renene.2017.04.001>.
- [16] A.E. Harman-Ware, et al., Microalgae as a renewable fuel source: fast pyrolysis of *scenedesmus* sp, *Renew. Energy* 60 (Dec. 2013) 625–632, <https://doi.org/10.1016/j.renene.2013.06.016>.
- [17] M. Faraji, M. Saidi, Hydrogen-rich syngas production via integrated configuration of pyrolysis and air gasification processes of various algal biomass: process simulation and evaluation using aspen plus software, *Int. J. Hydrogen Energy* 46 (36) (2021) 18844–18856, <https://doi.org/10.1016/j.ijhydene.2021.03.047>.
- [18] E.A.H. Zubaidy, D.M. Abouelnasr, Fuel recovery from waste oily sludge using solvent extraction, *Process Saf. Environ. Prot.* 88 (5) (Sep. 2010) 318–326, <https://doi.org/10.1016/j.psep.2010.04.001>.

- [19] A.P. Bora, D.P. Gupta, K.S. Durbha, Sewage sludge to bio-fuel: a review on the sustainable approach of transforming sewage waste to alternative fuel, *Fuel* 259 (Jan. 2020) 116262, <https://doi.org/10.1016/j.fuel.2019.116262>.
- [20] M. Shoaib Ahmed Khan, N. Grioui, K. Halouani, R. Benelmir, Techno-economic analysis of production of bio-oil from catalytic pyrolysis of olive mill wastewater sludge with two different cooling mechanisms, *Energy Convers. Manag.* X 13 (2022) 100170, <https://doi.org/10.1016/j.ecmx.2021.100170>.
- [21] K. Atsonios, K.D. Panopoulos, N. Nikolopoulos, A.A. Lappas, E. Kakaras, Integration of hydroprocessing modeling of bio-liquids into flowsheeting design tools for biofuels production, *Fuel Process. Technol.* 171 (2018) 148–161, <https://doi.org/10.1016/j.fuproc.2017.11.009>.
- [22] F. Motasemi, M.T. Afzal, A review on the microwave-assisted pyrolysis technique, *Renew. Sustain. Energy Rev.* 28 (Dec. 2013) 317–330, <https://doi.org/10.1016/j.rser.2013.08.008>.
- [23] X. Shi, et al., Investigating the synergistic driving action of microwave and char-based multi-catalysts on biomass catalytic pyrolysis into value-added bio-products, *Renew. Energy* 219 (Dec. 2023) 119490, <https://doi.org/10.1016/j.renene.2023.119490>.
- [24] J.J. Bolívar Caballero, I.N. Zaini, W. Yang, Reforming processes for syngas production: a mini-review on the current status, challenges, and prospects for biomass conversion to fuels, *Applications in Energy and Combustion Science* 10 (Jun. 2022) 100064, <https://doi.org/10.1016/j.jaecs.2022.100064>.
- [25] W. Jin, J.L. Santos, L. Pastor-Perez, S. Gu, M.A. Centeno, T.R. Reina, Noble metal supported on activated carbon for “Hydrogen Free” HDO reactions: exploring economically advantageous routes for biomass valorisation, *ChemCatChem* 11 (17) (2019) 4434–4441, <https://doi.org/10.1002/cctc.201900841>.
- [26] S. Caspani, F. Manenti, Hydrogen recovery from end-of-life tire pyrolysis gas via H₂S splitting, *Int. J. Hydrogen Energy* (Feb. 2025), <https://doi.org/10.1016/j.ijhydene.2025.02.059>.
- [27] M. Bozzini, K. Prifti, A. Galeazzi, F. Manenti, Capex opex robust optimization: a software for well-founded economic estimations and process optimization, *Chem. Eng. Trans.* 99 (May 2023) 619–624, <https://doi.org/10.3303/CET2399104>.
- [28] L.F. Sánchez, M.M. Bozzini, M. Vallerio, F. Manenti, A hybrid surrogate and simulation-based framework for efficient CapEx/OpEx optimization in complex chemical plants, *Chemical Engineering and Processing - Process Intensification* 219 (Jan. 2026) 110638, <https://doi.org/10.1016/j.cep.2025.110638>.
- [29] D. Fan, R. Yang, C. Chen, S. Qiu, S. He, H. Shi, Microwave catalytic co-pyrolysis of microalgae and high density polyethylene over activated carbon supported bimetallic: characteristics and bio-oil analysis, *Renew. Energy* 235 (Nov. 2024) 121323, <https://doi.org/10.1016/j.renene.2024.121323>.
- [30] B. Ruiz Bobes, D2.1 Physicochemical Sheet for the Biomass Feedstock, Oct. 2024 [Online]. Available: <https://zenodo.org/records/14163752>. (Accessed 8 April 2025).
- [31] J. Havlik, T. Dlouhý, Indirect dryers for biomass drying—comparison of experimental characteristics for drum and rotary configurations, *ChemEngineering* 4 (1) (Mar. 2020), <https://doi.org/10.3390/chemengineering4010018>.
- [32] X. Ren, et al., Challenges and opportunities in microwave-assisted catalytic pyrolysis of biomass: a review, *Appl. Energy* 315 (Jun. 2022) 118970, <https://doi.org/10.1016/j.apenergy.2022.118970>.
- [33] Z. Hu, Y. Zheng, F. Yan, B. Xiao, S. Liu, Bio-oil production through pyrolysis of blue-green algae blooms (BGAB): product distribution and bio-oil characterization, *Energy* 52 (Apr. 2013) 119–125, <https://doi.org/10.1016/j.energy.2013.01.059>.
- [34] K. Chaiwong, T. Kiatsiriroat, N. Vorayos, C. Thararax, Study of bio-oil and bio-char production from algae by slow pyrolysis, *Biomass Bioenergy* 56 (Sep. 2013) 600–606, <https://doi.org/10.1016/j.biombioe.2013.05.035>.
- [35] M. Adamczyk, M. Sajdak, Pyrolysis behaviours of microalgae *Nannochloropsis gaditana*, *Waste Biomass Valor.* 9 (11) (Nov. 2018) 2221–2235, <https://doi.org/10.1007/s12649-017-9996-8>.
- [36] M. Kwapinska, et al., Release of N-containing compounds during pyrolysis of milk/dairy processing sludge – experimental results and comparison of measurement techniques, *J. Anal. Appl. Pyrolysis* 178 (2024) 106391, <https://doi.org/10.1016/j.jaap.2024.106391>.
- [37] S. McIntosh, M.N. Nabi, L. Moghaddam, P. Brooks, P.S. Ghandehari, D. Erler, Combined pyrolysis and sulphided NiMo/Al₂O₃ catalysed hydroprocessing in a multistage strategy for the production of biofuels from milk processing waste, *Fuel* 295 (2021) 120602, <https://doi.org/10.1016/j.fuel.2021.120602>.
- [38] M.M. Bozzini, M. Signorelli, E. Moiola, F. Manenti, Techno-economic-assessment of the methanol synthesis from captured CO₂ and modular nuclear power-based electrolysis, *J. CO₂ Util.* 101 (Nov. 2025) 103186, <https://doi.org/10.1016/j.jcou.2025.103186>.
- [39] S. Saeidi, F. Fazlollahi, S. Najari, D. Iranshahi, J.J. Klemes, L.L. Baxter, Hydrogen production: perspectives, separation with special emphasis on kinetics of WGS reaction: a state-of-the-art review, *J. Ind. Eng. Chem.* 49 (May 2017) 1–25, <https://doi.org/10.1016/j.jiec.2016.12.003>.
- [40] M.M. Jaffar, M.A. Nahil, P.T. Williams, Synthetic natural gas production from the three stage (i) pyrolysis (ii) catalytic steam reforming (iii) catalytic hydrogenation of waste biomass, *Fuel Process. Technol.* 208 (Nov. 2020) 106515, <https://doi.org/10.1016/j.fuproc.2020.106515>.